JCB Article

Cortactin and Crk cooperate to trigger actin polymerization during *Shigella* invasion of epithelial cells

Laurence Bougnères,[1] Stéphane E. Girardin,[1] Scott A. Weed,[3] Andrei V. Karginov,[4] Jean-Christophe Olivo-Marin,[2] J. Thomas Parsons,[4] Philippe J. Sansonetti,[1] and Guy Tran Van Nhieu[1]

[1]Unité de Pathogénie Microbienne Moléculaire, INSERM U389 and [2]Unité d'Analyse d'Images Quantitative, Institut Pasteur, 75724 Paris Cedex 15, France
[3]Department of Craniofacial Biology, University of Colorado Health Sciences Center, Denver, CO 80262
[4]Department of Microbiology Health Sciences Center, University of Virginia, Charlottesville, VA 22908

Shigella, the causative agent of bacillary dysentery, invades epithelial cells in a process involving Src tyrosine kinase signaling. Cortactin, a ubiquitous actin-binding protein present in structures of dynamic actin assembly, is the major protein tyrosine phosphorylated during *Shigella* invasion. Here, we report that RNA interference silencing of cortactin expression, as does Src inhibition in cells expressing kinase-inactive Src, interferes with actin polymerization required for the formation of cellular extensions engulfing the bacteria. *Shigella* invasion induced the recruitment of cortactin at plasma membranes in a tyrosine phosphorylation–dependent manner. Overexpression of wild-type forms of cortactin or the adaptor protein Crk favored *Shigella* uptake, and Arp2/3 binding–deficient cortactin derivatives or an Src homology 2 domain Crk mutant interfered with bacterial-induced actin foci formation. Crk was shown to directly interact with tyrosine-phosphorylated cortactin and to condition cortactin-dependent actin polymerization required for *Shigella* uptake. These results point at a major role for a Crk–cortactin complex in actin polymerization downstream of tyrosine kinase signaling.

Introduction

Shigella flexneri, a gram-negative bacterium, causes bacillary dysentery in humans by invading the colonic epithelium and eliciting an intense inflammatory reaction that leads to destruction of this epithelium (Labrec et al., 1964; Sansonetti, 1998). Bacterial colonization of the mucosa depends on its ability to invade epithelial cells and to spread from cell to cell (Suzuki and Sasakawa, 2001). The ability of enteroinvasive pathogens such as *Shigella* to induce its internalization into cells that are normally nonphagocytic is a key event to its virulence. The "zipper"-like process used by *Yersinia* and *Listeria* is based on a high affinity interaction between a bacterial surface ligand and a host cell surface receptor, and implicates moderate cytoskeletal rearrangements (Gruenheid and Finlay, 2003). In contrast, the "triggering" process used by *Salmonella* and *Shigella* involves several bacterial factors and important rearrangements of the actin cytoskeleton leading to the formation of cell extensions that rise several micrometers above the cell surface and engulf the bacterium in a large vacuole (Galan, 2001). During the triggering process, a specialized type III secretion system determines the integration bacterial components into host cell membranes to form a so-called "translocon," which allows the subsequent delivery of type III effectors into the cell cytosol (Hueck, 1998). In the case of *Salmonella*, cytoskeleton reorganization is mediated by translocated type III effectors, the SopE and SptP proteins that act as a guanosine exchange factor and GTPase-activating protein toward the Rho GTPases Cdc42 and Rac, respectively (Galan, 2001). Although phenotypically similar, *Shigella* invasion implicates a different mechanism, as IpaC, a component of the translocon, triggers signals that lead to actin polymerization (Tran Van Nhieu et al., 1999). During the initial phase of *Shigella* entry, actin polymeriza-

The online version of this article includes supplemental material.

Address correspondence to G. Tran Van Nhieu, Unité de Pathogénie Microbienne Moléculaire, INSERM U389, Institut Pasteur, 28 rue du Dr. Roux, 75724 Paris Cedex 15, France. Tel.: (33) 1-45-68-83-15. Fax: (33) 1-45-68-89-53. email: gtranvan@pasteur.fr

Key words: *Shigella*; invasion; cortactin; Crk; actin

Abbreviations used in this paper: FL, full-length; p130Cas, p130 Crk-associated substrate; SH, Src homology; TM, tyrosine-mutated.

tion depends on Rho GTPases and Src tyrosine kinase activation, but the molecular links between these two pathways have not been identified (Duménil et al., 1998; Mounier et al., 1999). The Abl tyrosine kinase family was recently shown to be required for *Shigella* invasion and may provide such a link because Abl kinases are activated by Src and have been involved in F-actin dynamics (Plattner et al., 1999; Woodring et al., 2003). During *Shigella* invasion, Abl may activate Rho GTPases through phosphorylation of the Crk adaptor protein (Burton et al., 2003).

Another candidate that could link Rho GTPases and Src pathways is cortactin, an actin-binding protein recruited in *Shigella* entry foci, which is tyrosine phosphorylated in an Src kinase–dependent manner during *Shigella* entry (Wu et al., 1991; Dehio et al., 1995; Duménil et al., 1998). Cortactin distributes to sites of dynamic actin assembly, including lamellipodia, podosomes, and invadopodia (Wu and Parsons, 1993; Bowden et al., 1999).

Cortactin possesses a unique multidomain structure consisting of an acidic domain at the amino terminus (NTA) followed by 6.5 tandem repeats containing the F-actin binding site, a proline-rich region containing the three tyrosine residues (421, 466, and 482) that are phosphorylated by Src-related kinases (Huang et al., 1998), and a carboxy-terminal Src homology (SH) 3 domain. Cortactin binds to the Arp2/3 complex and stimulates its actin nucleation activity in vitro (Mullins et al., 1998; Weed et al., 2000; Uruno et al., 2001). Stimulation of cortactin-mediated actin nucleation is enhanced by its binding to F-actin (Uruno et al., 2001; Weaver et al., 2001) and to WIP, a protein involved in filopodia formation (Kinley et al., 2003). Binding to the Arp2/3 complex occurs through the cortactin tripeptide motif "DDW" located in its amino-terminal NTA domain, a motif that is conserved in many Arp2/3-binding/activating proteins such as HS1, Abp1, and WASP family proteins (Olazabal and Machesky, 2001). Cortactin-dependent actin nucleation may be relevant for the genesis of filopodial extensions such as dendritic spine (Hering and Sheng, 2003). Cortactin was also reported to prevent the debranching of Arp2/3–F-actin networks (Weaver et al., 2001).

Results

Cortactin is required for actin polymerization at the *Shigella* entry site and for efficient bacterial uptake

To inhibit cortactin expression, HeLa cells were transfected with an siRNA duplex corresponding to the 5′ sequence of the cortactin mRNA (dsRNA1). Immunofluorescence staining of transfected cells indicated that inhibition of cortactin expression was maximal 24 h after transfection of dsRNA1, with 74% of cells showing no detectable cortactin. Consistently, anti-cortactin Western blot analysis indicated a 70% decrease in cortactin levels in cells transfected with dsRNA1, compared with control samples (Fig. 1 a, cortactin), whereas no difference in the levels of expression of actin or Arp3

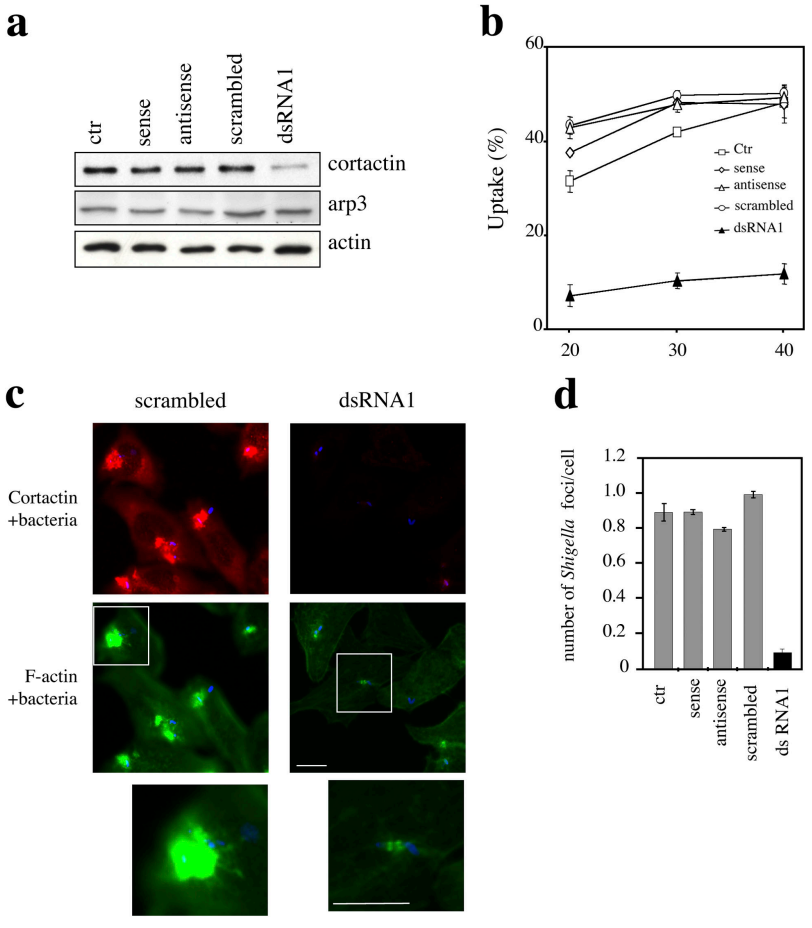

Figure 1. **Cortactin dsRNA interference inhibits *Shigella* entry.** HeLa cells were transfected with transfection reagent alone (ctr), sense and antisense strands of dsRNA1, scrambled version of dsRNA1 (scrambled), or dsRNA1. (a) 24 h after transfection, cell lysates were analyzed by Western blot using anti-cortactin (cortactin), anti-Arp3 (arp3), or anti-actin (actin) antibodies. A decrease in the cortactin levels was observed in dsRNA1-transfected cells in three independent experiments. (b–d) 24 h after transfection, cells were challenged with *Shigella*, fixed, and processed for staining. (b) Bacterial uptake was determined by differential outside/total bacteria immunofluorescence staining in the different controls and in dsRNA1-treated cells. (c) Representative fields of scrambled or dsRNA1-transfected cells challenged with *Shigella*; bacteria (blue), cortactin (red), and F-actin (green). Bottom panels correspond to higher magnification of the inset in the middle panels. Bars, 10 μm. (d) The frequency of F-actin foci formation was determined for each sample by counting foci in 600 cells. The plotted data were averaged from the scoring of samples from three independent experiments ± SEM.

could be detected (Fig. 1 a, arp3 and actin). F-actin staining indicated that cells transfected with dsRNA1 showed little modification of their actin cytoskeleton (unpublished data). The effects of cortactin inhibition on *Shigella* uptake were analyzed by infecting dsRNA1-treated cells with *Shigella*. As shown in Fig. 1 b, bacterial uptake in cells treated with dsRNA1 was decreased by fivefold compared with control cells. This decrease was still observed even after 40 min of bacterial challenge, showing that the invasion process was strongly inhibited in dsRNA1-treated cells and not simply delayed (Fig. 1 b). In dsRNA1-transfected cells, only weak actin polymerization was detected at the site of bacterial contact (Fig. 1 c), whereas as expected, massive actin polymerization was observed at entry sites in untransfected cells (unpublished data) or in scrambled dsRNA1-transfected cells (Fig. 1 c). The number of entry structures showing actin-rich extensions was decreased 10 times in dsRNA1-treated cells compared with control cells, as 90% of *Shigella*-induced structures in dsRNA1-treated cells appeared abortive (Fig. 1, c and d).

Conversely, overexpression of Flag-tagged full-length (FL) cortactin led to a twofold increase in bacterial uptake compared with mock cells (Fig. S1 and Fig. 2 a; online supplemental material available at http://www.jcb.org/cgi/content/full/jcb.200402073/DC1), with a 36% increase in the number of entry foci at 15 min in FL cells compared with mock cells (Fig. 2 b). FL cortactin was recruited in *Shigella*-induced cellular projections, and this recruitment was accompanied by increased actin polymerization (Fig. 2 c, compare FL and mock). When quantified (see Materials and methods), the surface area of F-actin foci in FL cells was on the average two times larger than in mock cells (Fig. 2 d), whereas the average intensity of the F-actin staining was not significantly different (Fig. 2 e; 60 actin foci, $n = 3$).

These results indicate that cortactin is essential for the development of the F-actin–rich cell projections that promote bacterial uptake.

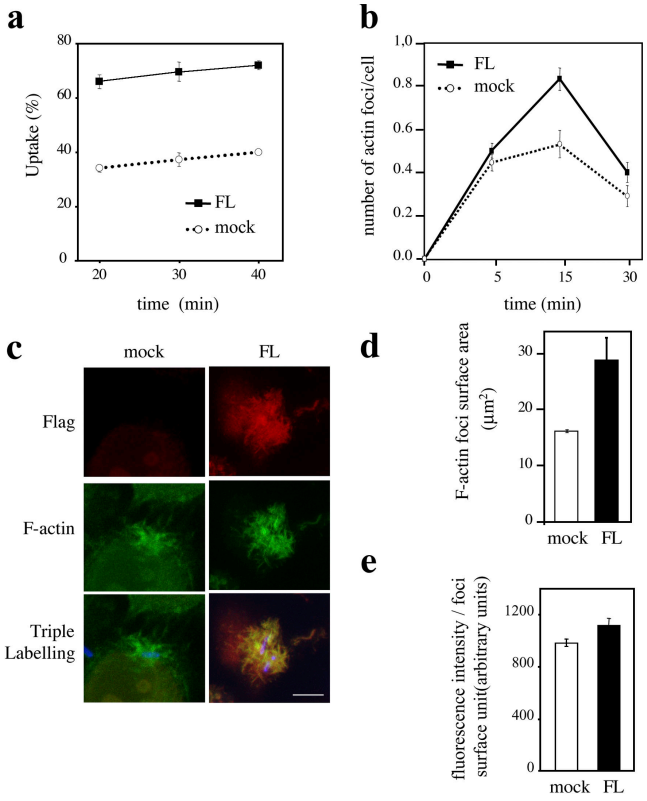

Figure 2. **Overexpression of cortactin enhances *Shigella*-induced actin polymerization and bacterial uptake.** HeLa cells were transfected with vector alone (mock) or Flag-tagged cortactin (FL). After 24 h, cells were infected with *Shigella*, fixed, and processed for fluorescent labeling. Transfected cells were visualized by staining of FL with anti-Flag antibody. (a) *Shigella* uptake is shown for mock cells (dotted line) and FL cells (solid line). (b) The frequency of *Shigella*-induced actin foci formation is shown for mock cells (dotted line) and FL cells (solid line). (c) Representative confocal images of *Shigella* foci observed in mock or FL cells, stained for Flag-tagged cortactin (red), F-actin (green), and *Shigella* (blue). Bar, 5 μm. (d and e) Quantitative analysis of the surface area and the fluorescence intensity per surface unit of F-actin foci was performed in mock cells (white bar) and FL cells (solid bar), using a dedicated computer program. All the plotted data shown in this figure were averaged from three independent experiments ± SEM.

Src-dependent tyrosine phosphorylation of cortactin regulates its localization and actin polymerization at *Shigella* entry sites

In cells stably overexpressing a kinase-inactive form of Src (SrcK− cells), the formation of *Shigella*-induced F-actin foci and tyrosine phosphorylation of cortactin were reported to be impaired (Duménil et al., 1998). To investigate if these two events were functionally linked, we analyzed cortactin distribution in *Shigella* entry structures induced in cells overexpressing a kinase-inactive form of Src (SrcK− cells). Confocal microscopy analysis indicated that in SrcK− cells, the majority of *Shigella*-induced structures showed F-actin staining limited to the intimate contact between the bacteria and the host cell membrane (Fig. 3 a, SrcK−), without massive actin polymerization such as those induced by *Shigella* in mock cells (Fig. 3 a, mock). Interestingly, in SrcK− cells, very few cortactin-rich extensions were observed as cortactin staining colocalized with F-actin staining at the immediate bacterial vicinity (Fig. 3 a, SrcK−). These observations were confirmed by quantifying the surface of *Shigella* F-actin foci in mock and SrcK− cells. As shown in Fig. 3 b, the foci average surface area delimited by F-actin staining in mock cells was threefold that measured in SrcK− cells (Fig. 3 b). These results indicate that Src activity is required for cortactin recruitment and actin polymerization in cell extensions surrounding the bacteria.

To determine the contribution of tyrosine phosphorylation of cortactin in actin foci formation, we used a Flag-tagged tyrosine-mutated (TM) cortactin with phenylalanine substituting for Tyr421, Tyr 466, and Tyr 482 (Huang et al., 1998). TM cortactin was expressed at similar levels to FL cortactin, which is approximately fourfold the level of endogenous cortactin, but in contrast to FL cortactin, TM cortactin was not phosphorylated upon *Shigella* invasion (Fig. S1, a and b). *Shigella*-induced F-actin foci were significantly smaller in TM cells than in mock cells (Fig. 3 a), with a nearly twofold reduction in size (Fig. 3 b) and a comparable density of F-actin staining at the site of bacteria–cell con-

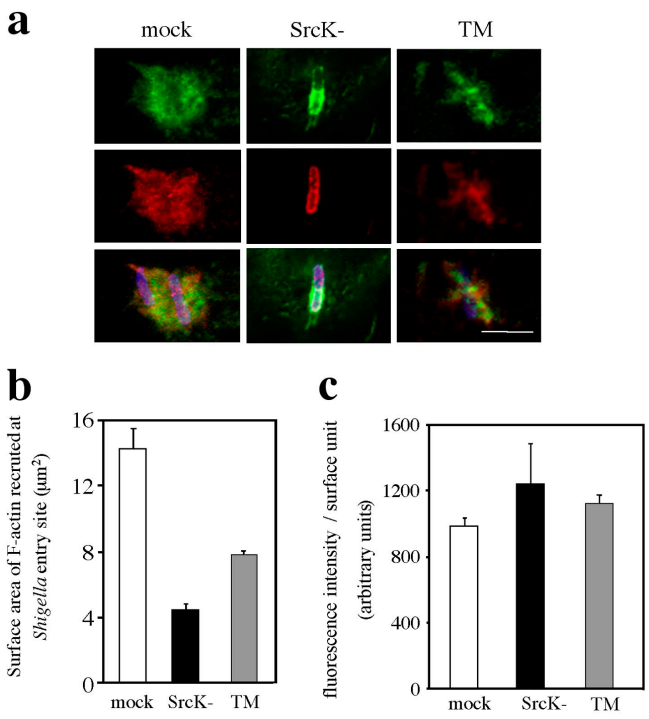

Figure 3. **Expression of kinase-inactive Src and TM cortactin inhibits *Shigella*-induced actin foci formation.** (a) Representative confocal microscopy images of *Shigella* entry structures observed in mock cells (mock), SrcK− cells (SrcK−), and cells expressing tyrosine-mutated cortactin (TM). Cells were challenged for 15 min with *Shigella*, fixed, and processed for fluorescence labeling of F-actin (green), cortactin (red), and bacterial LPS (blue). Bar, 5 μm. (b and c) Surface area and fluorescence intensity per surface unit of F-actin in *Shigella* entry structures were quantified in mock, SrcK−, and TM cells from images obtained with an epifluorescence microscope using a dedicated computer program (see Materials and methods). The analysis was performed on 60 foci from three independent experiments.

tact (Fig. 3 c). TM cortactin colocalized with F-actin (Fig. 3 a, TM) and endogenous cortactin (unpublished data) on a reduced area compared with mock cells.

These results indicate that Src-dependent tyrosine phosphorylation of cortactin regulates its localization and actin polymerization in cellular projections that surround the entering bacteria.

Cortactin associates with plasma membranes upon *Shigella* invasion

To analyze the distribution of cortactin during *Shigella* invasion, cellular membranes were fractionated by sucrose gradient sedimentation. Determination of the enzymatic activity of membrane markers indicated that plasma membranes were enriched in the 46% sucrose fraction (Fig. S2 a, available at http://www.jcb.org/cgi/content/full/jcb.200402073/DC1). Anti-cortactin Western blot analysis showed that cortactin predominantly distributed in the 34–39% sucrose fractions (Fig. 4 a). However, in cells infected with the invasive strain of *Shigella*, cortactin was consistently detected in the 46% sucrose fraction containing plasma membranes (Fig. 4 a; cortactin, INV). The cortactin shift was associated with a shift of actin, but not of tubulin, in the 46% sucrose fraction (Fig. 4 a, actin). Treatment with the detergent octyl-β-D-glucopyranoside that solubilizes membranes (Fig. S2 a, left) prevented detection of cortactin and actin in the 46% sucrose fraction (Fig. S2 b). To analyze if tyrosine phosphorylation was required for cortactin shift, fractionation experiments were performed in cells expressing FL or TM cortactin infected with *Shigella*. As shown in Fig. 4 b, and as observed for endogenous cortactin, FL cortactin mostly distributed in the 34–39% sucrose fractions and showed a shift in the plasma membrane–containing fraction when cells were infected with invasive *Shigella* (Fig. 4 b, FL). In contrast, TM cortactin was not detected in the plasma membrane–containing fraction (Fig. 4 b, TM). These results indicate that the cortactin shift toward plasma membranes depends on *Shigella*-induced tyrosine phosphorylation by Src. To further confirm this observation, HeLa cells were fluorescently surface labeled (see Materials and methods) before bacterial challenge and fractionation by sucrose gradient sedimentation. Immunofluorescence staining showed that on challenge with invasive *Shigella*, fluorescent spots corresponding to cortactin staining were detected in the 46% sucrose fraction that colocalized with membrane staining (Fig. S3, available at http://www.jcb.org/cgi/content/full/jcb.200402073/DC1). To demonstrate that cortactin not only colocalized but also associated with plasma membranes, plasma membrane–containing fractions were incubated with FITC-fluorescent beads coupled to anti-cortactin antibody. As shown in Fig. 4 c, bead and membrane clusters could be observed in samples challenged with invasive *Shigella* (Fig. 4 c). These clusters were not observed with uncoated beads (unpublished data) or with anti-cortactin beads in samples challenged with noninvasive *Shigella*, consistent with their formation being dependent on cortactin associating with membranes. As expected and as opposed to FL cortactin, TM cortactin did not colocalize with membranes of cells challenged with invasive *Shigella* and did not allow the formation of membrane clusters upon incubation with anti-Flag antibody-coated beads (Fig. S3, b and c). In control experiments, incubation of anti-α5β1 integrin antibody-coated beads led to the formation of membrane clusters in the 46% sucrose fraction (Fig. 4 c).

Altogether, these data demonstrate that on challenge with invasive *Shigella*, cortactin associates with plasma membranes in a tyrosine phosphorylation–dependent manner.

Mutation of the Arp2/3-binding site of cortactin impairs actin polymerization at the *Shigella* entry site

Cortactin has been reported to bind to and to activate the Arp2/3 complex (Weed et al., 2000; Uruno et al., 2001; Weaver et al., 2001), raising the possibility that it participates in actin polymerization within *Shigella*-induced cell extensions. We used cortactin mutants bearing point mutations in the NTA DDW motif (DD2021AA and W22A) that abolish the ability of cortactin to interact with the Arp2/3 complex. Cells transfected with these constructs were infected with *Shigella*, fixed, processed for fluorescence labeling, and analyzed by confocal microscopy. As shown in Fig. 5 a, these cortactin mutants were recruited at the entry structure with a localization similar to that of FL cortactin. These observa-

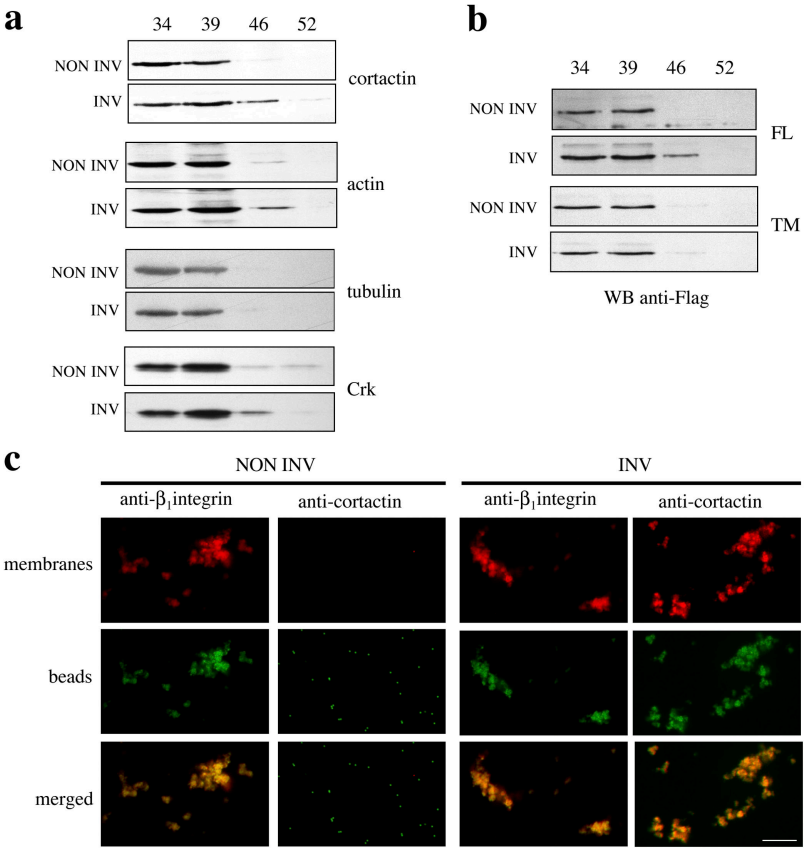

Figure 4. ***Shigella* invasion induces cortactin association with plasma membranes.** After challenge with noninvasive (NON INV) or invasive (INV) *Shigella*, cell extracts were fractionated using a discontinuous sucrose gradient. (a) Extracts from HeLa cells were fractionated and analyzed by anti-cortactin, anti-actin, anti-tubulin, and anti-Crk Western blot. Invasive *Shigella* induces a shift of cortactin to the plasma membrane–containing fraction. Actin and Crk co-shift with cortactin, but not with tubulin. (b) Extracts from cells transfected with full-length (FL) or tyrosine-mutated cortactin (TM) were fractionated and analyzed by anti-Flag Western blot. (c) Cells were surface labeled with a rhodamine derivative (red) previous to bacterial invasion. After cell extract fractionation on sucrose gradients, the plasma membrane–enriched 46% sucrose fraction was incubated with FITC-fluorescent beads (green) coupled to anti-cortactin or anti-β_1 integrin antibodies. Beads were recovered by centrifugation and fluorescence analysis was performed to determine the presence of plasma membranes. Bar, 5 μm.

tions indicate that the DD2021AA and W22A mutations do not prevent sublocalization of cortactin at a distance from the bacteria–cell intimate contact. In contrast, in DD2021AA or W22A transfectants, F-actin did not colocalize with mutated cortactin, and was only detected at the intimate contact of the bacteria (Fig. 5 a, DD2021AA and W22A). Very few actin-rich projections could be observed at the bacterial vicinity, and F-actin, detected as far as 6 μm above the bacteria in FL transfectants (Fig. 5 b, FL), was not detected further than 2 μm above the bacteria in DD2021AA or W22A transfectants (Fig. 5 b, DD2021AA and W22A). Quantitative analysis indicated that the number of *Shigella*-induced F-actin foci formed per cell in DD2021AA and W22A transfectants was only 20% that of actin foci formed in FL transfectants (Fig. 5 c; 600 cells, $n = 3$).

These results indicate that mutations that impair Arp2/3 binding to cortactin affect *Shigella*-induced actin-rich extensions, consistent with a concerted role for cortactin and Arp2/3 during bacterial entry.

Crk is recruited to membranes and associates with phosphorylated cortactin during *Shigella* invasion

Based on the finding that tyrosine phosphorylation of cortactin was required for its association with plasma membranes during *Shigella* invasion, we assumed that its membrane recruitment depended on interaction with SH2 domain–containing protein(s). Cortactin from v-Src transfectants was previously reported to associate with recombinant SH2 domains of Src, Nck, and Crk (Okamura and Resh, 1995). Cell fractionation experiments were performed to identify SH2 domain–containing proteins that cofractionate with cortactin in plasma membranes enriched fraction upon *Shigella* invasion. Western blot analysis of putative candidates showed no significant variation in the fractionation pattern of Src or Nck (unpublished data). In contrast, a significant shift of Crk was detected in the 46% plasma membrane–containing fraction on challenge with invasive *Shigella* (Fig. 4 a; Crk, INV). Immunofluorescence staining showed that Crk (Fig. 6 a, green) was recruited to *Shigella*-induced actin-rich extensions, where it colocalized with tyrosine-phosphorylated cortactin (Fig. 6 a, red).

To investigate a potential interaction of Crk with cortactin, FL cortactin was immunoprecipitated from extracts of cells challenged with *Shigella* (Fig. 6 b, anti-Flag). Western blot analysis showed that recombinant HA-Crk associated with cortactin (Fig. 6 b, anti-HA), but not with protein G–Sepharose alone. However, on challenge with invasive *Shigella*, Crk association with cortactin was enhanced by 1.8-fold when compared with noninvasive *Shigella* (Fig. 6 b, anti-HA). These data indicate that *Shigella* invasion induces cortactin association with Crk.

To determine if Crk directly binds to cortactin, cortactin overlay assays were performed using a purified GST-cortactin fusion (see Materials and methods). Crk was immunoprecipitated from HeLa cell lysates, fractionated by SDS-PAGE, and transferred to membrane filters. Strips from the same filter were probed first with GST-cortactin and GST. Protein binding was visualized using anti-GST mAb followed by standard immunodetection procedure (see Materials and methods). As shown in Fig. 6 c, GST-cortactin bound to a 40-kD protein

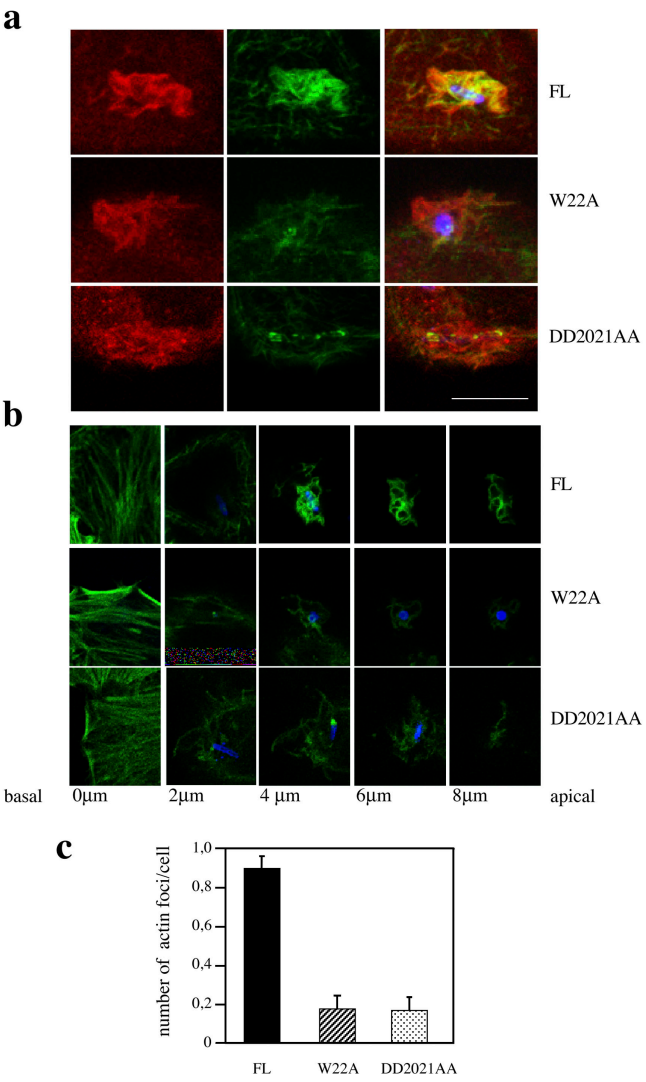

Figure 5. **Cortactin-dependent actin polymerization during *Shigella* entry requires the cortactin–Arp2/3 binding site.** (a and b) HeLa cells were transfected with wild-type cortactin (FL), the W22A cortactin mutant, or DD2021AA. 24 h after transfection, cells were challenged 15 min with *Shigella*, fixed, processed for fluorescence labeling, and analyzed by confocal microscopy. Samples were stained for exogenous cortactin (red), F-actin (green), and anti-LPS (blue). Bar, 5 μm. (b) Confocal planes of *Shigella* actin foci staining from the basal to apical region spaced by 2 μm. (c) The number of *Shigella*-induced actin foci per cell was determined from three independent experiments ± SEM. Mutations in the cortactin–Arp2/3 binding site impair the formation of *Shigella*-induced actin extensions.

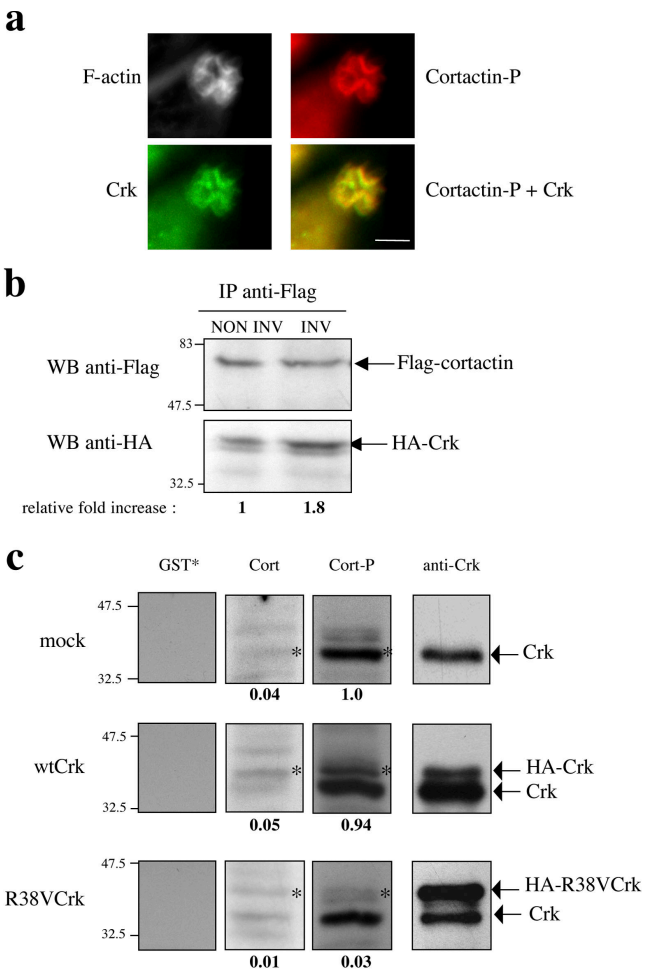

Figure 6. **Cortactin associates with Crk during *Shigella* entry.** (a) Cells were challenged 15 min with *Shigella*, fixed, and processed for fluorescence labeling of F-actin (gray), Crk (green), and tyrosine-phosphorylated cortactin (red). Images were acquired with an epifluorescence microscope. Bar, 5 μm. (b) FL cortactin was immunoprecipitated from HeLa cells coexpressing Flag-tagged cortactin and HA-tagged Crk, previously infected 15 min with noninvasive or invasive *Shigella*. Immune complexes were separated by SDS-PAGE, transferred to a membrane filter, and the same membrane was immunoblotted using anti-Flag or anti-HA antibodies, followed by ECL+ detection (Amersham Biosciences). For each sample, the relative fold increase corresponds to the intensity of the signal obtained for HA-Crk over that of Flag-cortactin, assigning the value "1" for the sample challenged with the noninvasive strain. (c) Immunoprecipitation from mock-, wtCrk-, or R38VCrk-transfected cell lysates using anti-Crk antibody was followed by gel electrophoresis. Anti-Crk Western blot analysis shows endogenous and recombinant Crk. Overlay analysis was performed using GST submitted to a kinase assay (GST*), GST-cortactin (Cort), or phosphorylated GST-cortactin (Cort-P) as probes. The bold number indicates the normalized value obtained for binding of cortactin or phosphorylated cortactin to bands labeled with an asterisk (see Materials and methods). Phosphorylated cortactin binds to endogenous or recombinant HA-Crk, but not to R38VCrk.

that co-migrated with endogenous Crk. To analyze the role of tyrosine phosphorylation of cortactin in regulating its direct binding to Crk, overlay assays were performed with GST-cortactin previously phosphorylated in vitro in an Src kinase assay (see Materials and methods). Anti-phosphotyrosine Western blot analysis indicated that as opposed to GST, GST-cortactin phosphorylation could be detected (Fig. S4, available at http://www.jcb.org/cgi/content/full/jcb.200402073/DC1). As shown in Fig. 6 c, binding to the 40-kD protein was significantly increased when cortactin was phosphorylated (Fig. 6 c; mock, GST-Cort-P). Binding of phosphorylated cortactin to the HA-tagged form of Crk (wt-Crk), which showed a shift in migration compared with endogenous Crk, was also detected (Fig. 6 c; wtCrk, GST-Cort-P). In contrast, when overlay assays were performed on an HA-tagged mutated form of Crk (R38VCrk) with the R38V

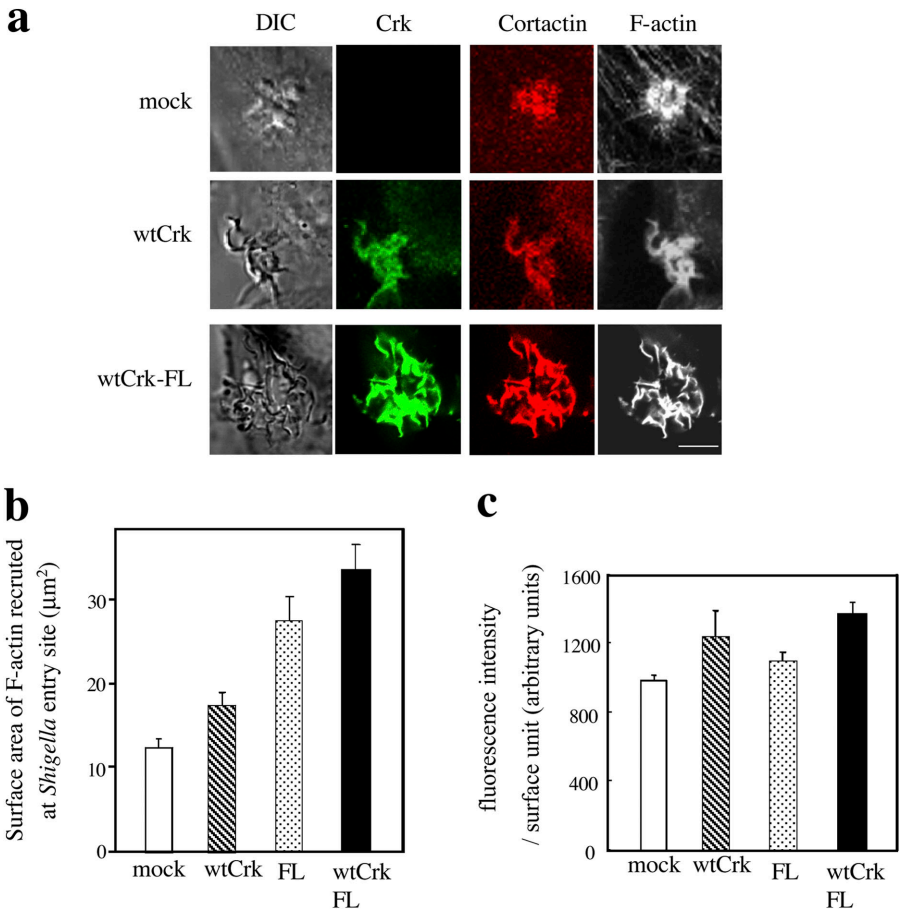

Figure 7. **Cortactin and Crk cooperate to stimulate the formation of *Shigella*-induced F-actin–rich extensions.** HeLa cells were transfected with vector alone (mock), Myc-tagged wild-type Crk (wtCrk), or FL cortactin (FL), or were cotransfected with Myc-tagged wild-type Crk and Flag-tagged FL cortactin (wtCrk-FL). (a) Representative confocal images of *Shigella* entry structures observed in mock transfectants, wtCrk transfectants, and wtCrk-FL cortactin cotransfectants. Cells were challenged 15 min with *Shigella*, fixed, and processed for fluorescence labeling of F-actin (black and white), Myc-Crk (green), and endogenous cortactin (red) in mock and wtCrk cells or of recombinant cortactin (red) in wtCrk-FL transfectants. Differential interference contrast (DIC) images show cell extension morphology at *Shigella* entry site. Bar, 5 μm. (b and c) Quantitative analysis of the surface area and the fluorescence intensity per surface unit of F-actin foci was performed in mock, wtCrk, FL, or wtCrk-FL transfectants using a dedicated computer program. Plotted data were averaged from three independent experiments ± SEM.

point mutation that alters the structure of its SH2 domain (Matsuda et al., 1992), little binding of phosphorylated GST-cortactin could be detected (Fig. 6 c; R38VCrk).

These data show that Crk directly interacts with tyrosine-phosphorylated cortactin, and that this interaction requires the Crk SH2 domain.

Functional evidence for a synergistic role of Crk and cortactin in *Shigella* uptake

To investigate the function of Crk during *Shigella* invasion, cells transfected with wtCrk were infected with *Shigella* and processed for immunofluorescence staining of recombinant Crk (Fig. 7, green), cortactin (Fig. 7, red), and F-actin (Fig. 7). Analysis of differential interference contrast images showed that *Shigella*-induced membrane projections were more developed in wtCrk cells than in mock cells, although the extent of actin polymerization was similar (Fig. 7 a, F-actin; Fig. 7 b). As observed for endogenous Crk, recombinant Crk colocalized with cortactin in *Shigella*-induced foci (Fig. 7 a). Similar to cells overexpressing FL cortactin, a 65% increase in the number of *Shigella*-induced foci per cell, accompanied with a 77% increase in *Shigella* uptake, was observed in wtCrk transfectants compared with mock cells (Fig. 8, a and b). This increase was specific for invasive *Shigella*, as noninvasive *Shigella* did not show detectable internalization in wtCrk cells (unpublished data).

When entry structures were analyzed in cells coexpressing wtCrk and FL cortactin, entry foci presented more projections but also showed a larger extent of actin polymerization compared with wtCrk or mock-transfected cells (Fig. 7 a, F-actin). Quantitative analysis indicated that the surface area of F-actin foci in wtCrk-FL cotransfectants was twofold higher than in cells overexpressing wtCrk alone (Fig. 7 b). The number of *Shigella*-induced F-actin foci per cell was twofold higher in wtCrk-FL cotransfectants compared with mock cells (Fig. 8 a), and 30% higher than in cells overexpressing wtCrk or FL cortactin alone (Fig. 8 a). In keeping with this, bacterial uptake was 2.4-fold higher in wtCrk-FL cotransfectants compared with mock cells (Fig. 8 b), with a 32% increase compared with wtCrk or FL cells (Fig. 8 b).

To investigate the consequences of the expression of the mutant form of Crk deficient for cortactin binding on *Shigella* uptake, cells transfected with R38VCrk were challenged with *Shigella*. In cells overexpressing R38VCrk, bacterial uptake was decreased by twofold (Fig. 8 b), with a 67% inhibition in the number of F-actin foci compared with mock cells (Fig. 8 a). Interestingly, a similar inhibition of actin foci and bacterial internalization was observed when R38VCrk was coexpressed with FL cortactin (Fig. 8, a and b), indicating that the stimulation of *Shigella* entry by cortactin requires a functional Crk SH2 domain.

Collectively, these data indicate that Crk and cortactin functionally cooperate to trigger *Shigella* invasion, presumably through a direct interaction between the Crk SH2 domain and phosphorylated cortactin.

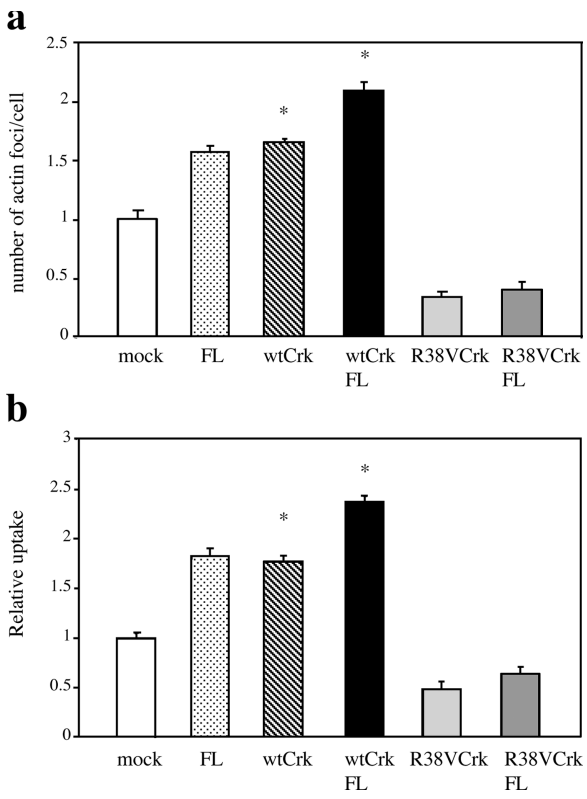

Figure 8. **Coupled action of Crk and cortactin is required for efficient uptake of *Shigella*.** HeLa cells were transfected with vector alone (mock), FL cortactin (FL), Myc-tagged wild-type Crk (wtCrk), or HA-tagged mutant Crk (R38VCrk), or were cotransfected with Myc-tagged wild-type Crk and Flag-tagged FL cortactin (wtCrk-FL), HA-tagged mutant Crk, and Flag-tagged FL cortactin (R38VCrk-FL). After 24 h of transfection, cells were infected with *Shigella*, fixed, and processed for fluorescent labeling. (a) The frequency of *Shigella*-induced actin foci formation at 15 min was scored for each transfectant. (b) *Shigella* uptake was determined for each transfectant using outside/total staining. The results of each experiment were normalized to the value obtained for mock transfectants, corresponding to 37% uptake. The average number of cell-associated bacteria was 4.5 bacteria per cell, and did not vary significantly in the different samples. The plotted data were averaged from the scoring of samples from three independent experiments ± SEM. Statistical significance was assessed by *t* test (denoted by asterisks).

Discussion

In this paper, we report that the knock-down of cortactin expression in HeLa cells by RNA interference leads to a dramatic decrease of *Shigella*-induced actin polymerization, with F-actin detected only at the intimate contact of the bacterial body. These resulting actin structures are inefficient to promote bacterial uptake. Conversely, in cells overexpressing cortactin, actin polymerization is amplified and cellular projections at a distance from the bacterial site of contact with the host cell membrane are increased, favoring F-actin foci development and *Shigella* uptake. Thus, cortactin participates in *Shigella* uptake by favoring actin polymerization and the formation of cellular extensions at the bacterial vicinity.

Because expression of cortactin mutants deficient for binding to Arp2/3 drastically reduces actin polymerization in *Shigella*-induced cellular projections, cortactin may directly participate in activation of the Arp2/3 complex. The observation that these cortactin mutants are still recruited within *Shigella*-induced cell extensions suggests that membrane recruitment and cortactin-dependent actin polymerization involve distinct molecular modules. In cells expressing inactive Src or a cortactin mutant deficient in tyrosine phosphorylation, cortactin localization is restricted to the intimate contact between the bacteria and the host cell membrane. This suggests that tyrosine phosphorylated by Src allows cortactin to localize to *Shigella*-induced projections and to determine actin polymerization. In this report, we demonstrate that *Shigella* invasion induces increased association of Crk and cortactin. Moreover, cortactin directly binds to Crk and tyrosine phosphorylation of cortactin enhances its binding. Thus, upon *Shigella* invasion, cortactin is likely to be recruited at the plasma membrane through direct interaction between tyrosine-phosphorylated residues and the Crk SH2 domain.

The Crk adaptor protein has been reported to modulate cell migration, a process that involves fine regulation of concomitant cell membrane extension/retraction and focal adhesion assembly/disassembly. Crk participates in these signaling cascades by connecting, through its SH2 or SH3 domains, upstream tyrosine-phosphorylated protein to downstream effectors implicated in the remodelling of the actin cytoskeleton. In many systems, p130 Crk-associated substrate (p130Cas) and paxillin are major partners interacting with Crk to mediate signal transmission from extracellular stimuli to reorganization of the actin cytoskeleton (Klemke et al., 1998; Cheresh et al., 1999). For example, upon ephrin-B1 stimulation of vascular endothelial cells, Crk relocalizes to focal complexes and its association with p130Cas mediates Rac activation, which leads to membrane ruffling (Nagashima et al., 2002). Paxillin is thought to function as a scaffold that organizes large signaling complexes at adhesion structures (Turner, 2000). In MDCK epithelial cells, HGF stimulation induces Crk association with paxillin and promotes Rac-dependent relocalization of paxillin to focal contacts (Lamorte et al., 2003). However, tyrosine phosphorylation of paxillin was reported to reduce integrin-mediated cell migration and transcellular invasive activities, whereas tyrosine phosphorylation of p130Cas may have opposite effects (Yano et al., 2000). Phosphorylation on Y221 of Crk negatively regulates binding to p130Cas and paxillin (Okada and Pessin, 1997; Takino et al., 2003). Interestingly, phosphorylation of Crk at Y221 appears to be required for membrane localization of Crk, which in turn leads to Rac membrane translocation and activation (Abassi and Vuori, 2002). Thus, the emerging concept is that Crk integrates multiple signals that could selectively lead to Crk-paxillin, Crk-p130Cas interaction, or Rac activation. Rac can mediate Arp2/3-dependent actin polymerization through interaction with IRSp53 and the WASP family protein WAVE (Miki et al., 2000). Rac was also reported to determine cortactin translocation to the cell cortex, where this latter could undergo sequential tyrosine phosphorylation (Weed et al., 1998; Head et al., 2003). Actin polymerization and membrane ruffling at the *Shigella* entry site require both Rac and cortactin. Inconsistent with the notion that cortactin would act only downstream of Rac, we present evidence that Crk directly interacts with cortactin during *Shigella* in-

vasion. Thus, Arp2/3-dependent actin polymerization in *Shigella*-induced cell extensions is likely to result from a combined activation of the Arp2/3 complex, mediated by cortactin and the Rac-WASP family protein pathway. This is in agreement with previous reports showing that cortactin and WASP family proteins act in concert to stimulate actin polymerization in vitro (Weaver et al., 2002; Uruno et al., 2003). According to these and other reports, upon activation, WASP family proteins activate Arp2/3-dependent actin polymerization and the association of Arp2/3 with actin filaments (Weaver et al., 2003). However, cortactin could stabilize the interaction of the Arp2/3 complex with the sides of actin filaments in a process involving a sequential interaction of cortactin and N-WASP with Arp2/3, or an N-WASP–cortactin–Arp2/3 ternary complex (Weaver et al., 2002; Uruno et al., 2003). This combined activity of N-WASP and cortactin could be critical for the formation of branched actin networks required for membrane ruffling at *Shigella* entry. Interestingly, cortactin dsRNA interference or expression of R38VCrk inhibited ruffle formation induced by active V12Rac, suggesting that cortactin and Crk stimulate actin polymerization downstream of Rac (Fig. S5, available at http://www.jcb.org/cgi/content/full/jcb.200402073/DC1). We propose that during *Shigella* invasion, Src activation leads to cortactin tyrosine phosphorylation and relocalization at the plasma membrane through an interaction with the Crk SH2 domain. Crk activation through phosphorylation of the tyrosine residue Y221, occurring downstream of the Abl kinase that may also result from Src activation (Plattner et al., 1999), would allow the membrane recruitment and the activation of Rac (Abassi and Vuori, 2002; Burton et al., 2003).

Materials and methods

Bacterial strains and cell lines

M90T, a wild-type strain of *S. flexneri* serotype 5, and the isogenic *mxiD* mutant deficient for type III secretion were described previously (Sansonetti et al., 1982; Allaoui et al., 1992). Expression of the AfaE adhesin (Garcia et al., 1996) was used to synchronize the infection process. HeLa cells were from American Type Culture Collection. SrcK− cell lines were described previously (Duménil et al., 1998).

Antibodies, reagents, and plasmids

Anti-cortactin 4F11, anti-phosphotyrosine 4G10, anti-GST mAb, and anti-Arp3 pAb were purchased from Upstate Biotechnology. Anti-cortactin pY421 pAb was purchased from Biosource International. Anti-*Shigella* LPS pAb was described previously (Mounier et al., 1997). Anti-Myc 9E10 mAb was from Santa Cruz Biotechnology, Inc.; anti-Flag M5 mAb and anti-actin pAb were purchased from Sigma-Aldrich. The anti-α5β1 integrin 6F11 mAb was described previously (Tran Van Nhieu and Isberg, 1991). Anti-tubulin mAb, anti–mouse IgG antibody coupled to Texas red, and anti–rabbit IgG antibody coupled to Cy5 were purchased from Amersham Biosciences. Anti-Crk mAb was purchased from BD Biosciences. Bodipy-labeled phallacidin and 5-TAMRA,SE were purchased from Molecular Probes, Inc. FITC fluorescent 0.75-μm microspheres were purchased from Polysciences, Inc.

Flag-tagged wild-type and triple-mutant (Y421F, Y466F, Y482F) cortactin constructs were described previously (Head et al., 2003). Myc-tagged cortactin constructs cloned in the BamH1 and EcoR1 sites of pRK5-Myc, containing substitutions of aspartic acid to alanine at residues 20 and 21 (DD2021AA), and of tryptophan to alanine at residue 22 (W22A) were generated from Myc-tagged wild-type cortactin gene using the QuikChange™ site-directed mutagenesis kit (QIAGEN). Myc-tagged Crk, HA-tagged Crk, and HA-CrkR38V were provided by Dr. M. Matsuda (Osaka University, Osaka, Japan). Myc-tagged V12Rac cloned into pRK5 was a gift from Dr. Alan Hall (University College of London, London, UK).

Transfection of cortactin siRNA duplexes

dsRNA1 resulted from annealing of a sense strand designed to match a sequence in 5′ of human cortactin mRNA and the anti-sense strand (sense 5′-GACUGAGAAGCAUGCCUCCdTdT-3′). The scrambled version of dsRNA1 corresponded to the sense strand 5′-ACGCGAGUCGACCAUGUCAdTdT-3′ and was tested for absence of matching with any GenBank DNA sequence.

HeLa cells were transfected using the jet SI™ reagent as indicated by the manufacturer's instructions (Eurogentec). For quantification analysis, samples corresponding to 100 μg of total proteins from 24 h transfected cell lysates were analyzed by anti-Arp3, anti-actin, and anti-cortactin Western blot, followed by ECL+ detection (Amersham Biosciences). Band intensities were determined by scanning the membrane using a PhosphorImager and were quantified using ImageQuant software (Molecular Dynamics).

Cell transfection

Transfection of HeLa cells, at 50% confluency, was performed using the cationic transfection reagent FuGENE™ (Boehringer Mannheim) with 1 μg of mock or cortactin cDNA encoding plasmids for 2×10^5 cells. After 24 h of transfection, immunoblotting, followed by densitometry analysis, was used to estimate the level of exogenous cortactin expression in transfected cells compared with endogenous cortactin expression in mock cells.

Immunofluorescence microscopy techniques

HeLa cells were infected with *Shigella* and prepared for immunofluorescence staining as described previously (Duménil et al., 1998). For *Shigella*-induced entry foci analysis, cells were first incubated with 10 U/ml Bodipy-phallacidin to label F-actin, anti-LPS pAb (1:1,000) to label bacteria, and with 5 μg/ml anti-cortactin mAb, 4.4 μg/ml anti-FLAG M5 mAb, or 5 μg/ml anti-Myc mAb. To check for the specificity of staining with the anti-phosphocortactin pY421 pAb, the antibody used at 2 μg/ml was incubated with 20 μg/ml purified GST-cortactin, or purified GST-cortactin subjected to in vitro Src phosphorylation for 30 min before use for immunofluorescence staining of fixed samples. Cells were then incubated with secondary antibodies coupled with fluorochromes (Cy5, Texas red). Bacterial uptake experiments were performed at 20, 30, and 40 min of invasion. In experiments with Crk transfectants, only the 20-min values are reported in the graph, given that the values at 20, 30, or 40 min of invasion were not significantly different. Uptake quantitation was achieved by staining of extracellular and total bacteria as described previously (Duménil et al., 1998). The relative amount of *Shigella* internalized in each transfectant was determined using the following quantitation: [total cell-associated bacteria − extracellular bacteria]/total bacteria. For transient transfection, only bacteria associated with transfected cells showing exogenous protein expression were scored. For each sample, 400 total bacteria were counted. All the plotted data shown were averaged from three independent experiments ± SEM. Statistical significance was assessed by *t* test.

Confocal microscopy analysis was performed using a confocal laser scanning microscope (LSM 510 Combi; Carl Zeiss MicroImaging, Inc.). Images were acquired with a 63× objective. Z-series of optical sections were performed at 1-μm increments.

Image analysis

Scoring of *Shigella*-induced actin foci and of bacterial internalization was performed with a 40× objective, using an epifluorescence microscope (DMRIBe; Leica) connected to a CCD camera (CoolSNAP HQ™; Princeton Instruments). Statistical quantification of the surface area and of the density of F-actin in bacterial-induced structures was achieved using a dedicated image analysis computer-assisted program. The procedure consists of thresholding the image to a value of fluorescence intensity under which pixels corresponding to the cellular background are not retained. The resulting binary mask is used to compute the surface and the density of protein recruitment as the average intensity of the fluorophore labeling per pixel unit. Quantification of cortactin staining to determine the levels of expression of recombinant proteins was achieved using a similar procedure under the MetaMorph® software (Universal Imaging corp.). All plotted data represent the analysis of 60 entry structures from three independent experiments. Statistical significance was assessed by *t* test.

Membrane fractionation of *Shigella*-infected HeLa cells

6×10^6 HeLa cells were infected with *Shigella* at a multiplicity of infection of 100:1 for 15 min. Cells were chilled on ice, washed in ice-cold PBS, scraped in homogenization buffer (20 mM Hepes, pH 7.4, 5 mM EDTA, 1 mM ABSF, antiproteases [COMPLETE; Boehringer], 2 mM $NaVO_3$, and 15% sucrose [wt/wt]), and homogenized in a 1-ml sml-Dounce (Kontes) with a pestle using 60 strokes. Samples were then centrifuged for 10 min at

3,000 *g*. The post-nuclear supernatant was collected, adjusted to 35% (wt/wt) sucrose, loaded over 1-ml cushions of 62 and 45% (wt/wt) sucrose solutions, and covered with 1 ml cushion of 15% (wt/wt) sucrose solution. Ultracentrifugation was performed in a swinging bucket rotor (model SW55; Beckman Coulter) for 2 h at 100,000 *g* at 4°C in an ultracentrifuge (model LE-80K; Beckman Coulter). Fractions of 0.5 ml were collected along the sucrose gradient. In the detergent experiment, octyl-β-D-glucopyranoside at 1 mM was used in all the solutions. The activity of the lysosomal enzyme *N*-acetyl-β-D-hexosaminidase was detected by incubating 50 μl of each collected fraction with 200 μl of 4.38 mM *p*-nitrophenyl *N*-acetyl-β-D-glucosaminide, 0.25% Triton X-100, and 50 mM citrate buffer, pH 5.0, for 3 h at 37°C and absorbance was read at 405 nm. The activity of plasma membrane alkaline phosphodiesterase was assayed by adding 50 μl of each collected fraction to 200 μl of 250 mM Tris, pH 9.0, 2.5 mM sodium thymidine 5′-monophosphate *p*-nitrophenyl ester (Sigma-Aldrich) for at least 6 h at 37°C and absorbance was read at 405 nm.

For immunofluorescence microscopy analysis of plasma membrane–containing fractions, cells were surface labeled with the rhodamine derivative 5-TAMRA,SE before bacterial challenge and cell fractionation on sucrose gradients.

Overlay assay

Crk was immunoprecipitated from cell lysates of HeLa cells, or HeLa cells transfected with HA-wtCrk or HA-CrkR38V. Immunoprecipitates were subjected to SDS-PAGE on a gel containing 10% polyacrylamide and transferred onto an Immobilon™-P filter (Millipore). Filters were blocked in PBS containing 2% BSA (Sigma-Aldrich). GST and GST-cortactin fusion were subjected to an in vitro Src kinase assay. 1 μg of GST or GST-cortactin, expressed in *Escherichia coli* and purified by affinity chromatography, was incubated with 1 μl of Src (p60c-Src), corresponding to 3 U of recombinant enzyme expressed in Sf9 insect cells (Upstate Biotechnology), in 20 μl kinase buffer (50 mM Hepes, pH 7.4, 10 mM $MgCl_2$, and 1 mM ATP). Samples were incubated at 37°C for 10 min with gentle agitation, samples were analyzed by SDS-PAGE, and tyrosine phosphorylation was visualized by anti-phosphotyrosine Western blot. In overlay assays, GST or GST-cortactin was used at a final concentration of 0.5 μg protein/ml in PBS-T to probe filters for 1 h at RT. Filters were washed three times in PBS-T and incubated with an anti-GST mAb at 0.5 μg/ml in PBS-T for 1 h to detect binding of GST fusion proteins. Bound antibodies were detected by incubation with anti–mouse IgG coupled to HRP. After washing, bound proteins were detected using the ECL+ system (Amersham Biosciences), and the signal intensity was quantified using a PhosphorImager (Storm; Molecular Dynamics). Normalized cortactin-binding values were calculated as the following: values obtained for binding of cortactin or phosphorylated cortactin in the overlay assays were normalized over that determined for the amount of the corresponding form of Crk by anti-Crk Western blot analysis. The number "1" was arbitrarily assigned to the normalized valued obtained for cortactin binding to endogenous Crk.

Online supplemental material

Fig. S1 (a) shows the quantification of FL or TM cortactin staining intensity in HeLa cell transfectants. Fig. S1 (b) shows anti-phosphotyrosine Western blot analysis of lysates of cell transfectants expressing FL or TM, challenged with *Shigella*. Fig. S2 (a and b) shows the effects of octylglucopyranoside treatment on membrane fractionation on sucrose gradients, and on cortactin and actin detection in the 46% sucrose fraction. Fig. S3 (a) shows colocalization of cortactin with fluorescently labeled membranes in the 46% sucrose fraction of samples challenged with invasive *Shigella*, and Fig. S3 (b) the lack of membrane colocalization of TM. Fig. S3 (c) shows membrane clustering induced by anti-Flag antibody incubation of membrane fractions of FL (but not TM) transfectants. Fig. S4 (a) corresponds to anti-pY421 Western blot analysis showing cross-reactivity of a cortactin co-migrating band in samples challenged with invasive *Shigella*. Fig. S4 (b) shows depression of *Shigella*-induced actin foci immunofluorescence staining upon preincubation of the pY421 pAb with in vitro–phosphorylated cortactin. Fig. S5 shows the effects of cortactin siRNA interference and R38V Crk expression on V12Rac-induced actin polymerization and membrane ruffles. Online supplemental material available at http://www.jcb.org/cgi/content/full/jcb.200402073/DC1.

We thank Javier Pizarro-Cerda for technical help with sucrose gradients. We thank Thomas Meyer for helpful suggestions with siRNA experiments.

L. Bougnères received a fellowship from the French Ministry of Higher Education and Research and from the Fondation pour la Recherche Médicale. P.J. Sansonetti is a Howard Hughes Medical Institute Scholar.

Submitted: 13 February 2004
Accepted: 28 May 2004

References

Abassi, Y.A., and K. Vuori. 2002. Tyrosine 221 in Crk regulates adhesion-dependent membrane localization of Crk and Rac and activation of Rac signaling. *EMBO J.* 21:4571–4582.

Allaoui, A., P.J. Sansonetti, and C. Parsot. 1992. MxiJ, a lipoprotein involved in secretion of *Shigella* Ipa invasins, is homologous to YscJ, a secretion factor of the Yersinia Yop proteins. *J. Bacteriol.* 174:7661–7669.

Bowden, E.T., M. Barth, D. Thomas, R.I. Glazer, and S.C. Mueller. 1999. An invasion-related complex of cortactin, paxillin and PKCμ associates with invadopodia at sites of extracellular matrix degradation. *Oncogene.* 18:4440–4449.

Burton, E.A., R. Plattner, and A.M. Pendergast. 2003. Abl tyrosine kinases are required for infection by *Shigella flexneri*. *EMBO J.* 22:5471–5479.

Cheresh, D.A., J. Leng, and R.L. Klemke. 1999. Regulation of cell contraction and membrane ruffling by distinct signals in migratory cells. *J. Cell Biol.* 146: 1107–1116.

Dehio, C., M.C. Prevost, and P.J. Sansonetti. 1995. Invasion of epithelial cells by *Shigella flexneri* induces tyrosine phosphorylation of cortactin by a pp60c-src-mediated signaling pathway. *EMBO J.* 14:2471–2482.

Duménil, G., J.C. Olivo, S. Pellegrini, M. Fellous, P.J. Sansonetti, and G.T. Nhieu. 1998. Interferon α inhibits a Src-mediated pathway necessary for *Shigella*-induced cytoskeletal rearrangements in epithelial cells. *J. Cell Biol.* 143:1003–1012.

Galan, J.E. 2001. *Salmonella* interactions with host cells: type III secretion at work. *Annu. Rev. Cell Dev. Biol.* 17:53–86.

Garcia, M.I., P. Gounon, P. Courcoux, A. Labigne, and C. Le Bouguenec. 1996. The afimbrial adhesive sheath encoded by the afa-3 gene cluster of pathogenic *Escherichia coli* is composed of two adhesins. *Mol. Microbiol.* 19:683–693.

Gruenheid, S., and B.B. Finlay. 2003. Microbial pathogenesis and cytoskeletal function. *Nature.* 422:775–781.

Head, J.A., D. Jiang, M. Li, L.J. Zorn, E.M. Schaefer, J.T. Parsons, and S.A. Weed. 2003. Cortactin tyrosine phosphorylation requires Rac1 activity and association with the cortical actin cytoskeleton. *Mol. Biol. Cell.* 14:3216–3229.

Hering, H., and M. Sheng. 2003. Activity-dependent redistribution and essential role of cortactin in dendritic spine morphogenesis. *J. Neurosci.* 23:11759–11769.

Huang, C., J. Liu, C.C. Haudenschild, and X. Zhan. 1998. The role of tyrosine phosphorylation of cortactin in the locomotion of endothelial cells. *J. Biol. Chem.* 273:25770–25776.

Hueck, C.J. 1998. Type III protein secretion systems in bacterial pathogens of animals and plants. *Microbiol. Mol. Biol. Rev.* 62:379–433.

Kinley, A.W., S.A. Weed, A.M. Weaver, A.V. Karginov, E. Bissonette, J.A. Cooper, and J.T. Parsons. 2003. Cortactin interacts with WIP in regulating Arp2/3 activation and membrane protrusion. *Curr. Biol.* 13:384–393.

Klemke, R.L., J. Leng, R. Molander, P.C. Brooks, K. Vuori, and D.A. Cheresh. 1998. CAS/Crk coupling serves as a "molecular switch" for induction of cell migration. *J. Cell Biol.* 140:961–972.

Labrec, E.H., H. Schneider, T.J. Magnani, and S.B. Formal. 1964. Epithelial cell penetration as an essential step in the pathogenesis of bacillary dysentery. *J. Bacteriol.* 88:1503–1518.

Lamorte, L., S. Rodrigues, V. Sangwan, C.E. Turner, and M. Park. 2003. Crk associates with a multimolecular Paxillin/GIT2/β-PIX complex and promotes Rac-dependent relocalization of Paxillin to focal contacts. *Mol. Biol. Cell.* 14:2818–2831.

Matsuda, M., S. Tanaka, S. Nagata, A. Kojima, T. Kurata, and M. Shibuya. 1992. Two species of human CRK cDNA encode proteins with distinct biological activities. *Mol. Cell. Biol.* 12:3482–3489.

Miki, H., H. Yamaguchi, S. Suetsugu, and T. Takenawa. 2000. IRSp53 is an essential intermediate between Rac and WAVE in the regulation of membrane ruffling. *Nature.* 408:732–735.

Mounier, J., F.K. Bahrani, and P.J. Sansonetti. 1997. Secretion of *Shigella flexneri* Ipa invasins on contact with epithelial cells and subsequent entry of the bacterium into cells are growth stage dependent. *Infect. Immun.* 65:774–782.

Mounier, J., V. Laurent, A. Hall, P. Fort, M.F. Carlier, P.J. Sansonetti, and C. Egile. 1999. Rho family GTPases control entry of *Shigella flexneri* into epithelial cells but not intracellular motility. *J. Cell Sci.* 112:2069–2080.

Mullins, R.D., J.A. Heuser, and T.D. Pollard. 1998. The interaction of Arp2/3 complex with actin: nucleation, high affinity pointed end capping, and formation of branching networks of filaments. *Proc. Natl. Acad. Sci. USA.* 95: 6181–6186.

Nagashima, K., A. Endo, H. Ogita, A. Kawana, A. Yamagishi, A. Kitabatake, M. Matsuda, and N. Mochizuki. 2002. Adaptor protein Crk is required for ephrin-B1-induced membrane ruffling and focal complex assembly of human aortic endothelial cells. *Mol. Biol. Cell.* 13:4231–4242.

Okada, S., and J.E. Pessin. 1997. Insulin and epidermal growth factor stimulate a conformational change in Rap1 and dissociation of the CrkII-C3G complex. *J. Biol. Chem.* 272:28179–28182.

Okamura, H., and M.D. Resh. 1995. p80/85 cortactin associates with the Src SH2 domain and colocalizes with v-Src in transformed cells. *J. Biol. Chem.* 270: 26613–26618.

Olazabal, I.M., and L.M. Machesky. 2001. Abp1p and cortactin, new "handholds" for actin. *J. Cell Biol.* 154:679–682.

Plattner, R., L. Kadlec, K.A. DeMali, A. Kazlauskas, and A.M. Pendergast. 1999. c-Abl is activated by growth factors and Src family kinases and has a role in the cellular response to PDGF. *Genes Dev.* 13:2400–2411.

Sansonetti, P.J. 1998. Pathogenesis of shigellosis: from molecular and cellular biology of epithelial cell invasion to tissue inflammation and vaccine development. *Jpn. J. Med. Sci. Biol.* 51(Suppl):S69–S80.

Sansonetti, P.J., D.J. Kopecko, and S.B. Formal. 1982. Involvement of a plasmid in the invasive ability of *Shigella flexneri*. *Infect. Immun.* 35:852–860.

Suzuki, T., and C. Sasakawa. 2001. Molecular basis of the intracellular spreading of Shigella. *Infect. Immun.* 69:5959–5966.

Takino, T., M. Tamura, H. Miyamori, M. Araki, K. Matsumoto, H. Sato, and K.M. Yamada. 2003. Tyrosine phosphorylation of the CrkII adaptor protein modulates cell migration. *J. Cell Sci.* 116:3145–3155.

Tran Van Nhieu, G., and R.R. Isberg. 1991. The Yersinia pseudotuberculosis invasin protein and human fibronectin bind to mutually exclusive sites on the $\alpha_5\beta_1$ integrin receptor. *J. Biol. Chem.* 266:24367–24375.

Tran Van Nhieu, G., E. Caron, A. Hall, and P.J. Sansonetti. 1999. IpaC induces actin polymerization and filopodia formation during Shigella entry into epithelial cells. *EMBO J.* 18:3249–3262.

Turner, C.E. 2000. Paxillin and focal adhesion signaling. *Nat. Cell Biol.* 2:E231–E236.

Uruno, T., J. Liu, P. Zhang, Y. Fan, C. Egile, R. Li, S.C. Mueller, and X. Zhan. 2001. Activation of Arp2/3 complex-mediated actin polymerization by cortactin. *Nat. Cell Biol.* 3:259–266.

Uruno, T., J. Liu, Y. Li, N. Smith, and X. Zhan. 2003. Sequential interaction of actin-related proteins 2 and 3 (Arp2/3) complex with neural Wiscott-Aldrich syndrome protein (N-WASP) and cortactin during branched actin filament network formation. *J. Biol. Chem.* 278:26086–26093.

Weaver, A.M., A.V. Karginov, A.W. Kinley, S.A. Weed, Y. Li, J.T. Parsons, and J.A. Cooper. 2001. Cortactin promotes and stabilizes Arp2/3-induced actin filament network formation. *Curr. Biol.* 11:370–374.

Weaver, A.M., J.E. Heuser, A.V. Karginov, W.L. Lee, J.T. Parsons, and J.A. Cooper. 2002. Interaction of cortactin and N-WASp with Arp2/3 complex. *Curr. Biol.* 12:1270–1278.

Weaver, A.M., M.E. Young, W.L. Lee, and J.A. Cooper. 2003. Integration of signals to the Arp2/3 complex. *Curr. Opin. Cell Biol.* 15:23–30.

Weed, S.A., Y. Du, and J.T. Parsons. 1998. Translocation of cortactin to the cell periphery is mediated by the small GTPase Rac1. *J. Cell Sci.* 111:2433–2443.

Weed, S.A., A.V. Karginov, D.A. Schafer, A.M. Weaver, A.W. Kinley, J.A. Cooper, and J.T. Parsons. 2000. Cortactin localization to sites of actin assembly in lamellipodia requires interactions with F-actin and the Arp2/3 complex. *J. Cell Biol.* 151:29–40.

Woodring, P.J., T. Hunter, and J.Y. Wang. 2003. Regulation of F-actin-dependent processes by the Abl family of tyrosine kinases. *J. Cell Sci.* 116:2613–2626.

Wu, H., and J.T. Parsons. 1993. Cortactin, an 80/85-kilodalton pp60src substrate, is a filamentous actin-binding protein enriched in the cell cortex. *J. Cell Biol.* 120:1417–1426.

Wu, H., A.B. Reynolds, S.B. Kanner, R.R. Vines, and J.T. Parsons. 1991. Identification and characterization of a novel cytoskeleton-associated pp60src substrate. *Mol. Cell. Biol.* 11:5113–5124.

Yano, H., H. Uchida, T. Iwasaki, M. Mukai, H. Akedo, K. Nakamura, S. Hashimoto, and H. Sabe. 2000. Paxillin α and Crk-associated substrate exert opposing effects on cell migration and contact inhibition of growth through tyrosine phosphorylation. *Proc. Natl. Acad. Sci. USA.* 97:9076–9081.